Multipath Mitigation for GNSS Positioning in an Urban Environment Using Sparse Estimation

Julien Lesouple, *Student Member, IEEE*, Thierry Robert, Mohamed Sahmoudi, Jean-Yves Tourneret, *Senior Member, IEEE*, and Willy Vigneau

***Abstract*— Multipath (MP) remains the main source of error when using global navigation satellite systems (GNSS) in a constrained environment, leading to biased measurements and thus to inaccurate estimated positions. This paper formulates the GNSS navigation problem as the resolution of an overdetermined system whose unknowns are the receiver position and speed, clock bias and clock drift, and the potential biases affecting GNSS measurements. We assume that only a part of the satellites are affected by MP, i.e., that the unknown bias vector has several zero components, which allows sparse estimation theory to be exploited. The natural way of enforcing this sparsity is to introduce an ℓ_1 regularization associated with the bias vector. This leads to a least absolute shrinkage and selection operator problem that is solved using a reweighted-ℓ_1 algorithm. The weighting matrix of this algorithm is designed carefully as functions of the satellite carrier-to-noise density ratio (C/N_0) and the satellite elevations. Experimental validation conducted with real GPS data show the effectiveness of the proposed method as long as the sparsity assumption is respected.**

***Index Terms*— GNSS, multipath mitigation, sparse, LASSO, reweighted-l1 algorithm.**

I. Introduction

MULTIPATH (MP) is one of the most difficult error sources that needs to be tackled for GNSS positioning [2], [3]. Indeed, MP signals are generally due to reflections on various obstacles, and thus strongly depend on the geometric configuration of the scene in which the receiver is located. More precisely, in the absence of obstacle, the receiver is not affected by MP. Conversely, when the receiver is located close to buildings, the received GNSS measurements are very likely to be subjected to MP. The problem of mitigating MP effects in GNSS measurements has received a considerable attention in the literature. MP can be mitigated at the antenna level, by exploiting the fact that reflections change the polarization of the received signals. As a consequence, antennas can be designed to be more sensitive to the right polarization [4], [5]. Another important characteristic of reflected signals is their low or negative elevation that can be used at the antenna level to attenuate MP signals [4], [5]. Methods using antenna arrays also exist [6]–[8]. A recent technique combines the two latest methods mentioned [9]. MP can also be mitigated at the receiver level, by modifying the correlator, e.g., by using narrow correlators [10], double delta correlators [11], early late slope [12] or vision correlators [13]. Other techniques work at the discriminator level, such as the Maximum likelihood techniques based on an MP estimating delay lock loop (MEDLL) [14]–[16], the coupled amplitude DLL (CADLL) [17], or the Multipath Insensitive DLL (MIDLL) [18] have also been developed for MP signals. All the previously mentioned techniques need specific and expensive hardware that cannot always be purchased. Mitigating MP at a measurement or position level is thus an interesting alternative. A first solution is to take advantage of a 3D model of the environment to predict MP signals [19]–[23], and even to combine these techniques to other sensors, such as cameras. However, this 3D model is not always available in practical applications. A second option is to use the information available at the receiver, such as pseudoranges, Doppler shifts, satellite ephemeris and C/N_0. A widespread technique is to smooth the code measurements with phase measurements that are more robust to MP [24]. Other techniques consist in exploiting different measurements from the same satellite, for instance code and phase measurements leading to the code minus carrier (CmC) [4], or the difference between the measurements from two receivers leading to differential GNSS [5] or even from two different users (collaborative or cooperative positioning) [25], [26]. An interesting family of MP mitigation methods rely on statistical tests trying to exclude or correct the faulty measurements. The receiver autonomous integrity monitoring (RAIM) method belongs to this class of strategies [27], [28]. More recent technique uses a-contrario modeling for discarding bad satellites [29]. Note that these techniques require redundant measurements, that are not always available in urban environment, and that the user will only be able to detect/estimate up to two faulty measurements. Other techniques consider non-gaussian error terms, such as Gaussian mixtures, Markov process [30] or Dirichlet process mixtures [31], [32].

The point of view considered in this work is to model the effect of MP signals on GNSS measurements as additive

Manuscript received September 13, 2017; revised February 5, 2018; accepted June 5, 2018. This work was supported in part by the CNES and in part M3 Systems. The Associate Editor for this paper was C. F. Mecklenbräuker. *(Corresponding author: Julien Lesouple.)*

J. Lesouple is with the TéSA Laboratory, 31500 Toulouse, France (e-mail: julien.lesouple@tesa.prd.fr).

T. Robert is with the Centre national d'études spatiales, 31400 Toulouse, France.

M. Sahmoudi is with the ISAE, University of Toulouse, 31400 Toulouse, France (e-mail: mohamed.sahmoudi@isae.fr).

J.-Y. Tourneret is with the TéSA, IRIT, ENSEEIHT, University of Toulouse, 31071 Toulouse, France (e-mail: jean-yves.tourneret@enseeiht.fr).

W. Vigneau is with M3 Systems, 31410 Lavernose-Lacasse, France.

Color versions of one or more of the figures in this paper are available online at http://ieeexplore.ieee.org.

Digital Object Identifier 10.1109/TITS.2018.2848461

biases as in [33]. These biases have then to be estimated and subtracted from the GNSS measurements to mitigate MP effects. Sequential Monte Carlo methods also referred to as particle filters were investigated in [33] for this estimation. However, these methods are computationally intensive, making a real time implementation very complicated in practical applications. The main contribution of this paper is to exploit sparse estimation theory to estimate these biases with a significantly reduced computational complexity. The main hypothesis making this theory applicable is that many satellites are not affected by MP making the biases sparse with respect to number of received measurements. Note that sparse estimation for mitigating multipath has already been considered in Radar theory [34], [35], and that sparse assumption was also considered for GNSS applications in [36]. However, the proposed approach is different. It results from the application of a penalized least squares approach method taking advantage of the recent developments in sparse estimation theory. Since the measurement equation is linear with respect to the state vector, we estimate it directly from the data and the biases term in order to form a profile likelihood that is used to estimate the MP biases. This sparse estimation formulation avoids to consider an augmented state vector for bias estimation as in [36]. Instead, the bias vector is directly obtained by the minimization of a a penalized least-squares criterion resulting from a sparse MP prior.

This paper is organized as follows: Section II summarizes some basic principles on satellite navigation, describing how measurements (code measurements and Doppler rates) are related to the state vector (position, velocity) and the possible MP biases. This section also recalls the Kalman filtering steps that will be used to track the receiver position. Section III summarizes the main ideas of sparse estimation theory and the main estimation methods (LASSO, reweighted-ℓ_1 and generalized LASSO) that can be used to estimate sparse vectors. Section IV presents our contributions, i.e., how to estimate MP biases using GNSS measurements with some sparsity constraints. More precisely, we propose to consider a linearized navigation equation and to assign some sparsity constraints on the biases possibly affecting GNSS measurements. The positioning problem is then formulated as a penalized least squares problem with an ℓ_1 regularization inspired by the reweighted-ℓ_1 algorithm [37]. However, contrary to [37], the weighting matrix used in this work is designed using important information available at the receiver, based on the value of the carrier-to-noise density ratio (C/N_0) and the satellite positions. Experiments are presented in Section V comparing the proposed algorithm with other navigation strategies (Kalman filter, robust Kalman filter, classical LASSO, coded filter [36]). Conclusions and future work are reported in Section VI.

II. GNSS Fundamentals

A. Observation Model

The navigation problem considered in GNSS consists in estimating the position of a receiver from signals sent by different satellites. More precisely, measuring the propagation delay between the receiver and a given satellite, the receiver is able to build a so-called pseudorange defined as follows [38]

$$\rho^i = \|\boldsymbol{x}^i - \boldsymbol{x}_u\|_2 + b + \varepsilon^i \tag{1}$$

where

- ρ^i denotes the pseudorange between the receiver and the ith satellite, with $i \in \{1, \ldots, N\}$, N being the number of in-view satellites,
- $\boldsymbol{x}_u = (x, y, z)^T$ is the receiver position to be estimated,
- $\boldsymbol{x}^i = (x^i, y^i, z^i)^T$ is the known ith satellite position,
- $\|\boldsymbol{x}^i - \boldsymbol{x}_u\|_2 = \sqrt{(x^i - x)^2 + (y^i - y)^2 + (z^i - z)^2}$ is the distance between the user and the ith satellite,
- b is the receiver clock bias, common to all measurements (hence the name of pseudorange),
- ε^i is the error term associated with the ith propagation canal (modeling ionospheric delay, tropospheric delay, satellite clock bias, satellite position uncertainty, MP and receiver noise).

A classical way of estimating the receiver position from N measurement equations as defined in (1) is to use an iterative algorithm, which linearizes (1) around the previous computed position. The resulting linearized problem for GNSS navigation can be classically expressed as [39] and [40]

$$\boldsymbol{y}_p = \boldsymbol{G}\boldsymbol{x} + \boldsymbol{m}_p + \boldsymbol{n}_p \tag{2}$$

with

- $\boldsymbol{y}_p \in \mathbb{R}^N$ the difference between the measured and estimated pseudoranges (the subscript p is used for pseudoranges),
- $\boldsymbol{G} \in \mathbb{R}^{N\times 4}$ the Jacobian matrix associated with the linearized system,
- $\boldsymbol{x} \in \mathbb{R}^4$ the difference between the state (position and receiver clock bias) estimated at the previous position and the current state value,
- $\boldsymbol{m}_p \in \mathbb{R}^N$ an error term due to the possible presence of MP affecting the pseudoranges (we assume that all errors except MP have been corrected),
- $\boldsymbol{n}_p \sim \mathcal{N}(\boldsymbol{0}, \boldsymbol{R}_p) \in \mathbb{R}^N$ a zero-mean Gaussian noise vector with covariance matrix $\boldsymbol{R}_p$.

The expression of the matrix $\boldsymbol{G}$ can be found in many textbooks such as [39] and is recalled here for completeness

$$\boldsymbol{G} = \begin{bmatrix} a_1^1 & a_2^1 & a_3^1 & 1 \\ a_1^2 & a_2^2 & a_3^2 & 1 \\ \vdots & \vdots & \vdots & \vdots \\ a_1^N & a_2^N & a_3^N & 1 \end{bmatrix} \tag{3}$$

with

$$\left[a_1^i,\, a_2^i,\, a_3^i\right]^T = \frac{\boldsymbol{x}_0 - \boldsymbol{x}^i}{\|\boldsymbol{x}_0 - \boldsymbol{x}^i\|} \tag{4}$$

where $\boldsymbol{x}_0$ is the point around which (1) has been linearized.

After differentiating (1), the following result can be obtained [39]

$$\dot{\rho}^i = \left[a_1^i,\, a_2^i,\, a_3^i\right](\dot{\boldsymbol{x}}_u - \dot{\boldsymbol{x}}^i) + \dot{b} + \dot{\varepsilon}^i \tag{5}$$

which leads to the following linear equation that is associated with pseudorange rates and is very similar to (2)

$$\boldsymbol{y}_r = \boldsymbol{G}\dot{\boldsymbol{x}} + \boldsymbol{m}_r + \boldsymbol{n}_r \tag{6}$$

where

- $\boldsymbol{y}_r \in \mathbb{R}^N$ is the difference between the measured and estimated pseudorange rate (the subscript r is used to indicate pseudorange rates),
- $\dot{\boldsymbol{x}} \in \mathbb{R}^4$ is the difference between the state (velocity and receiver clock drift) estimated at the previous position and the current state value,
- $\boldsymbol{m}_r \in \mathbb{R}^N$ is an error term due to the possible presence of MP affecting the pseudorange rate,
- $\boldsymbol{n}_r \sim \mathcal{N}(\boldsymbol{0}, \boldsymbol{R}_r) \in \mathbb{R}^N$ is a zero-mean Gaussian noise vector with covariance matrix $\boldsymbol{R}_r$.

The main idea investigated in this paper is to exploit the property that few satellites are suffering from MP such that $\boldsymbol{m} = (\boldsymbol{m}_p, \boldsymbol{m}_r)^T$ is a sparse vector, i.e., a vector containing a lot of zeroes. As a consequence, sparse estimation theory can be used to estimate $\boldsymbol{m}$ and $\boldsymbol{x}$ jointly. Note that the terms $\boldsymbol{m}_p$ and $\boldsymbol{m}_r$ in (2) and (6) are both resulting from the possible presence of MP. However, as the receiver computes these two measurements differently, there is a priori no relation between these two terms. Before providing more details about the proposed sparse estimation method, we recall some basic elements about the extended Kalman filter that will be used for state estimation.

B. Extended Kalman Filter for GNSS

The EKF considered in this work is very classical and has been studied in many papers or textbooks including, e.g. [41, p. 195] or [42]. The state vector at time instant k, denoted as $\boldsymbol{s}_k$ (for $k = 1, \ldots, K$, where K is the sample size), contains the receiver position and velocity expressed in the ECEF frame, and the clock bias and drift (derivative of clock bias), i.e.,

$$\boldsymbol{s}_k = \left[x_k, \dot{x}_k, y_k, \dot{y}_k, z_k, \dot{z}_k, b_k, \dot{b}_k\right]^T \tag{7}$$

where

- the subscript k denotes the time instant,
- $(x_k, y_k, z_k)^T$ is the receiver position at time instant k,
- $(\dot{x}_k, \dot{y}_k, \dot{z}_k)^T$ is the receiver velocity at time instant k,
- b_k is the clock bias at time instant k,
- $\dot{b}_k$ is the clock drift at time instant k.

The relationship between the state vectors $\boldsymbol{s}_k$ and $\boldsymbol{s}_{k-1}$, is defined by a propagation equation that is used to design the Kalman filter. Let's denote

$$\boldsymbol{C}_k = \begin{bmatrix} 1 & \Delta t_k \\ 0 & 1 \end{bmatrix} \tag{8}$$

and

$$\boldsymbol{F}_k = \begin{bmatrix} \boldsymbol{C}_k & \boldsymbol{0}_{2\times2} & \boldsymbol{0}_{2\times2} & \boldsymbol{0}_{2\times2} \\ \boldsymbol{0}_{2\times2} & \boldsymbol{C}_k & \boldsymbol{0}_{2\times2} & \boldsymbol{0}_{2\times2} \\ \boldsymbol{0}_{2\times2} & \boldsymbol{0}_{2\times2} & \boldsymbol{C}_k & \boldsymbol{0}_{2\times2} \\ \boldsymbol{0}_{2\times2} & \boldsymbol{0}_{2\times2} & \boldsymbol{0}_{2\times2} & \boldsymbol{C}_k \end{bmatrix}. \tag{9}$$

The propagation equation considered in this work is

$$\boldsymbol{s}_k = \boldsymbol{F}_{k-1}\boldsymbol{s}_{k-1} + \boldsymbol{u}_{k-1} \tag{10}$$

with

- $\boldsymbol{F}_k$ the state transition matrix at time instant k,
- Δt_k the duration between two consecutive measurements,
- $\boldsymbol{u}_{k-1} \sim \mathcal{N}(\boldsymbol{0}, \boldsymbol{Q}_{k-1})$ the process noise at time instant $k-1$, supposed to be zero-mean Gaussian with known covariance matrix $\boldsymbol{Q}_{k-1}$ (see [43] for a closed-form expression).

The receiver can have access to various measurements depending on the application. In this paper, we focus on the code pseudorange (ρ^i) and the Doppler rate (Δf^i), even if the proposed methodology is quite general and can be applied to any kind of measurement affected by sparse additive biases. Assuming that the receiver has access to N satellite signals ($N > 4$), the measurement vector can be defined as

$$\begin{bmatrix} \boldsymbol{\rho} \\ \dot{\boldsymbol{\rho}} \end{bmatrix} = \left[\rho^1, \ldots, \rho^N, \dot{\rho}^1, \ldots, \dot{\rho}^N\right]^T \tag{11}$$

where $\dot{\rho}^i = -\lambda_{L_1}\Delta f^i$ is the ith pseudorange rate, with λ_{L_1} the wavelength of the received signal. As explained in Section II-A, the measurements are related to the state vector thanks to (2) and (6) and can be concatenated into a single equation defined as

$$\boldsymbol{y}_k = \boldsymbol{H}_k\boldsymbol{x}_k + \boldsymbol{m}_k + \boldsymbol{n}_k \tag{12}$$

where

- $\boldsymbol{y}_k \in \mathbb{R}^{2N}$ contains the difference between the actual and predicted pseudoranges and pseudorange rates at time k,
- $\boldsymbol{H}_k$ is the joint observation matrix for pseudoranges and pseudorange rates at time k (see technical report [43] for a closed-form expression),
- $\boldsymbol{x}_k = \boldsymbol{s}_k - \hat{\boldsymbol{s}}_k \in \mathbb{R}^8$ is the difference between the state vector (receiver position, velocity, clock bias, and clock drift) estimated at the previous position and the current state vector at time k,
- $\boldsymbol{m}_k \in \mathbb{R}^{2N}$ is a bias term due to the possible presence of MP at time k,
- $\boldsymbol{n}_k \sim \mathcal{N}(\boldsymbol{0}, \boldsymbol{R}_k) \in \mathbb{R}^{2N}$ is a zero-mean Gaussian noise vector at time k with covariance matrix $\boldsymbol{R}_k$ (see technical report [43] for a closed-form expression).

The classical EKF used to estimate the state vector from the state equation (10) and the measurement equations (1) and (5) can be summarized as follows

1) one step prediction
   $\hat{\boldsymbol{s}}_{k|k-1} = \boldsymbol{F}_{k-1}\hat{\boldsymbol{s}}_{k-1|k-1}$
2) one step prediction error covariance
   $\boldsymbol{P}_{k|k-1} = \boldsymbol{F}_{k-1}\boldsymbol{P}_{k-1|k-1}\boldsymbol{F}_{k-1}^T + \boldsymbol{Q}_{k-1}$
3) Kalman gain
   $\boldsymbol{K}_k = \boldsymbol{P}_{k|k-1}\boldsymbol{H}_k^T\left(\boldsymbol{H}_k\boldsymbol{P}_{k|k-1}\boldsymbol{H}_k^T + \boldsymbol{R}_k\right)^{-1}$
4) state estimation
   $\hat{\boldsymbol{s}}_{k|k} = \hat{\boldsymbol{s}}_{k|k-1} + \boldsymbol{K}_k\boldsymbol{y}_k$
5) state error covariance
   $\boldsymbol{P}_{k|k} = (I - \boldsymbol{K}_k\boldsymbol{H}_k)\,\boldsymbol{P}_{k|k-1}$.

In this paper, we have adopted the square root implementation of the Kalman filter discussed in [41, p. 181] for its known robustness.

Remark: In order to compensate for relativistic effects, time group delays and clock biases for the different satellites, we followed [44]. Ionospheric delays and their derivatives

were compensated using the well known Klobuchar model [45]. Zenith values were computed as in [46] and mapped with the Niell global mapping function [47] to remove the effects of tropospheric delays and their derivatives. Based on these compensations, the residual error was considered as Gaussian centered with variance $\sigma^2_{UERE} = \sigma^2_{Ephemeris} + \sigma^2_{Iono} + \sigma^2_{Tropo} + \sigma^2_{Clock}$ *for the pseudoranges and* $\dot{\sigma}^2_{UERE} = \dot{\sigma}^2_{Ephemeris} + \dot{\sigma}^2_{Iono} + \dot{\sigma}^2_{Tropo} + \dot{\sigma}^2_{Clock}$ *for pseudorange rates, see [39, p. 326] for justification and [39, p. 273] for typical values. However, other additive biases due for instance to errors in ionospheric or tropospheric corrections can also affect the received measurements as additive biases. The proposed method will include these errors in the vector* $\boldsymbol{m}_k$ *and will correct them, providing the sparsity assumption is satisfied.*

III. Sparse Estimation Theory

This section recalls the principles of sparse estimation theory and the main algorithms that can be used to estimate sparse vectors. Assume that we have a vector of measurements $\tilde{\boldsymbol{y}} \in \mathbb{R}^{2N}$ defined as $\tilde{\boldsymbol{y}} = \tilde{\boldsymbol{H}}\boldsymbol{\theta} + \tilde{\boldsymbol{n}}$, where $\tilde{\boldsymbol{H}} \in \mathbb{R}^{2N\times q}$ is a known regression matrix, $\boldsymbol{\theta} \in \mathbb{R}^q$ is an unknown sparse vector (to be estimated) and $\tilde{\boldsymbol{n}} \in \mathbb{R}^{2N}$ is an unknown error term.[1] A classical way of estimating $\boldsymbol{\theta}$ from the observed measurement vector $\tilde{\boldsymbol{y}}$ is to consider a data fidelity term $\frac{1}{2}\|\tilde{\boldsymbol{y}} - \tilde{\boldsymbol{H}}\boldsymbol{\theta}\|_2^2$ penalized by an additive regularization promoting the sparsity of $\boldsymbol{\theta}$. One can think of defining this additive regularization as the ℓ_0 pseudo-norm of $\boldsymbol{\theta}$ defined by

$$\|\boldsymbol{\theta}\|_0 = \#\{\theta_i \neq 0, i = 1, \ldots, q\}. \tag{13}$$

This problem can be formulated in different ways [48] and we choose the unconstrained one defined by

$$\hat{\boldsymbol{\theta}} = \underset{\boldsymbol{\theta}\in\mathbb{R}^q}{\operatorname{argmin}} \frac{1}{2}\|\tilde{\boldsymbol{y}} - \tilde{\boldsymbol{H}}\boldsymbol{\theta}\|_2^2 + \lambda\|\boldsymbol{\theta}\|_0 \tag{14}$$

where $\lambda \in \mathbb{R}$ is a fixed constant referred to as regularization parameter. However, the problem (14) is NP-hard and non-convex. Therefore, many relaxations have been proposed in the literature to bypass this difficulty, as summarized below.

A. The LASSO Problem

A classical way of estimating a sparse vector from a linear regression is to replace the ℓ_0 pseudo-norm in (14) by an ℓ_1 norm, i.e., to consider the so-called LASSO problem [49]

$$\underset{\boldsymbol{\theta}\in\mathbb{R}^q}{\operatorname{argmin}} \frac{1}{2}\|\tilde{\boldsymbol{y}} - \tilde{\boldsymbol{H}}\boldsymbol{\theta}\|_2^2 + \lambda\|\boldsymbol{\theta}\|_1. \tag{15}$$

However, algorithms used to solve this problem can provide solutions that are far from the solution of (14) [37]. This has motivated the study of many different sparse estimation strategies described in the next sections.

[1]The meaning of the different vectors $\tilde{\boldsymbol{y}}, \boldsymbol{\theta}, \tilde{\boldsymbol{n}}$ in the GNSS context will be clarified in Section IV.

B. The Reweighted-ℓ_1l1 and the Generalized LASSO

Candès *et al.* [37] investigated a so-called reweighted-ℓ_1 method defined as follows

$$\underset{\boldsymbol{\theta}\in\mathbb{R}^q}{\operatorname{argmin}} \frac{1}{2}\|\tilde{\boldsymbol{y}} - \tilde{\boldsymbol{H}}\boldsymbol{\theta}\|_2^2 + \lambda\|\boldsymbol{W}\boldsymbol{\theta}\|_1 \tag{16}$$

where $\boldsymbol{W} \in \mathbb{R}^{q\times q}$ is a diagonal weighting matrix. Ideally, the weights contained in $\boldsymbol{W}$ should be inversely proportional to the magnitude of the true unknown vector $\boldsymbol{\theta}_0$, i.e., such that

$$w_i = \begin{cases} \frac{1}{|\theta_{0,i}|}, & \theta_{0,i} \neq 0, \\ \infty, & \theta_{0,i} = 0. \end{cases} \tag{17}$$

However, this weight definition cannot be used in practice since $\boldsymbol{\theta}_0$ is an unknown vector. One solution proposed by Candès *et al.* [37] is summarized in the following iterative algorithm

1) set $\ell = 0$ and $w_i^{(0)} = 1, i = 1, \ldots, q$,
2) solve the problem

$$\boldsymbol{\theta}^{(\ell)} = \underset{\boldsymbol{\theta}\in\mathbb{R}^q}{\operatorname{argmin}} \frac{1}{2}\|\tilde{\boldsymbol{y}} - \tilde{\boldsymbol{H}}\boldsymbol{\theta}\|_2^2 + \lambda\|\boldsymbol{W}^{(\ell)}\boldsymbol{\theta}\|_1, \tag{18}$$

3) update the weights as

$$w_i^{(\ell+1)} = \frac{1}{|\theta_i^{(\ell)}| + \varepsilon}, \tag{19}$$

4) end when ℓ reaches a maximum value $\ell_{\max}$.

This algorithm requires to adjust the two parameters ε and $\ell_{\max}$. An adhoc choice was suggested in [37], namely $\varepsilon = 0.1$ and $\ell_{\max} = 2$.

A generalized version of (15) referred to as "generalized LASSO" was introduced in [50]

$$\underset{\boldsymbol{\theta}\in\mathbb{R}^q}{\operatorname{argmin}} \frac{1}{2}\|\tilde{\boldsymbol{y}} - \tilde{\boldsymbol{H}}\boldsymbol{\theta}\|_2^2 + \lambda\|\boldsymbol{W}\boldsymbol{\theta}\|_1 \tag{20}$$

where $\boldsymbol{W} \in \mathbb{R}^{p\times q}$ is an appropriate penalty matrix that is not necessarily square (p denotes the number of constraints associated with the unknown parameter vector $\boldsymbol{\theta}$) and needs to be specified by the user. Of course, when $p = q$ and $\boldsymbol{W}$ is diagonal, the generalized LASSO reduces to the reweighted-ℓ_1 method.

IV. A New Multipath Mitigation Method for GNSS

A. Problem Formulation

The proposed MP mitigation method assumes that the bias vector $\boldsymbol{m} = (\boldsymbol{m}_p, \boldsymbol{m}_r)^T$ resulting from (2) and (6) is sparse. Exploiting this sparsity property, we propose to solve the following problem

$$\underset{\boldsymbol{x},\boldsymbol{m}}{\operatorname{argmin}} \frac{1}{2}\|\boldsymbol{y} - \boldsymbol{H}\boldsymbol{x} - \boldsymbol{m}\|_2^2 + \lambda\|\boldsymbol{W}\boldsymbol{m}\|_1 \tag{21}$$

in order to detect and correct measurements affected by MP, i.e., measurements affected by the presence of additive biases. Note that these corrected measurements will be used as input of the EKF presented in II-B. In order to obtain a formulation similar to (16), it is interesting to note that the minimization

of (21) with respect to $\boldsymbol{x}$ for a fixed $\boldsymbol{m}$ admits a closed-form expression defined by

$$\boldsymbol{x} = (\boldsymbol{H}^T\boldsymbol{H})^{-1}\boldsymbol{H}^T(\boldsymbol{y}-\boldsymbol{m}) \tag{22}$$

which is the classical least squares solution. After replacing this expression of $\boldsymbol{x}$ in (21), we obtain the so-called profile likelihood

$$L(\boldsymbol{m}) = \frac{1}{2}\|(I_{2N}-\boldsymbol{P})(\boldsymbol{y}-\boldsymbol{m})\|_2^2 + \lambda\|\boldsymbol{W}\boldsymbol{m}\|_1 \tag{23}$$

where I_{2N} is the $2N \times 2N$ identity matrix and $\boldsymbol{P}$ is the following projection matrix

$$\boldsymbol{P} = \boldsymbol{H}(\boldsymbol{H}^T\boldsymbol{H})^{-1}\boldsymbol{H}^T. \tag{24}$$

Remark: It is interesting to note that the matrix $\boldsymbol{P}$ is a projection matrix associated with the subspace spanned by the columns of $\boldsymbol{H}$, denoted as $\text{Vec}\{\boldsymbol{H}\} = \{\boldsymbol{y} \in \mathbb{R}^{2N}, \exists \boldsymbol{x} \in \mathbb{R}^8, \boldsymbol{y} = \boldsymbol{H}\boldsymbol{x}\}$. As a consequence, the matrix $I_{2N} - \boldsymbol{P}$ in (23) is the projection matrix on the orthogonal of $\text{Vec}\{\boldsymbol{H}\}$. Recalling the observation equation

$$\boldsymbol{y} = \boldsymbol{H}\boldsymbol{x} + \boldsymbol{m} + \boldsymbol{n} \tag{25}$$

we can observe that the profile likelihood estimates the bias vector $\boldsymbol{m}$, by projecting the bias-corrected measurements $\boldsymbol{y}-\boldsymbol{m}$ onto the orthogonal of $\boldsymbol{H}$, which makes sense, since it is clearly impossible to distinguish the bias components located in $\text{Vec}\{\boldsymbol{H}\}$ from the term $\boldsymbol{H}x$.

After introducing the following notations

$$\tilde{\boldsymbol{y}} = (I_{2N}-\boldsymbol{P})\boldsymbol{y} \tag{26}$$

$$\tilde{\boldsymbol{H}} = (I_{2N}-\boldsymbol{P})\boldsymbol{W}^{-1} \tag{27}$$

$$\boldsymbol{\theta} = \boldsymbol{W}\boldsymbol{m} \tag{28}$$

the original problem (21) reduces to

$$\underset{\boldsymbol{\theta}\in\mathbb{R}^q}{\text{argmin}}\ \frac{1}{2}\|\tilde{\boldsymbol{y}} - \tilde{\boldsymbol{H}}\boldsymbol{\theta}\|_2^2 + \lambda\|\boldsymbol{\theta}\|_1 \tag{29}$$

where we have to note that $\boldsymbol{\theta} = \boldsymbol{W}\boldsymbol{m}$ is a sparse vector as the weighting matrix $\boldsymbol{W}$ is diagonal. As a consequence, we have to solve a LASSO problem whose solution can be obtained using classical efficient algorithms [49], [51], [52] and an example of algorithm is given in [43] from [53]. The resulting MP mitigation strategy can be summarized as follows

1) estimate the unknown parameter vector $\boldsymbol{\theta}$ as the solution of the LASSO problem (29) yielding $\hat{\boldsymbol{\theta}}$,
2) estimate the bias vector as $\hat{\boldsymbol{m}} = \boldsymbol{W}^{-1}\hat{\boldsymbol{\theta}}$,
3) correct the pseudorange and pseudorange rate measurements by removing the estimated bias vector to the pseudorange and pseudorange rates (i.e., $\boldsymbol{y} \leftarrow \boldsymbol{y} - \hat{\boldsymbol{m}}$). These corrected measurements are then processed using the EKF described in Section II-B.

B. Choosing the Weighting Matrix

A major issue, which is an important contribution of this work, is to design the weighting matrix appearing in (21). In this paper, we propose to build the weighting matrix $\boldsymbol{W}$ using some key parameters, somehow representative of the measurements quality, provided by most GNSS receivers, namely the carrier-to-noise density ratio C/N_0 [40] and the satellite elevations (that reflect the good or bad positions of the different satellites). More precisely, we want to consider a reweighted-ℓ_1 method favoring satellites with large C/N_0 values (the higher C/N_0, the better, as the tracking noise is reduced) and high satellite elevations (the higher the elevation, the better, as linked to the C/N_0 and tracking noise, and as less subject to multipath). Of course, there are several ways of building weights in agreement with these two considerations. For the parameter C/N_0, we propose to consider the approach suggested in [54] using the following weighting function

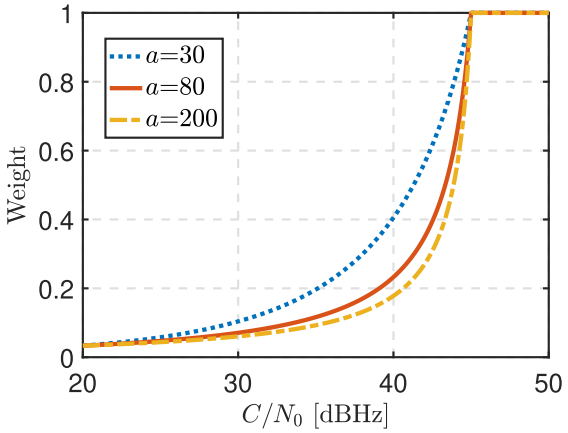

Fig. 1. Weighting function $w_1(C/N_0)$ for various values of a ($A = 30$, $F = 20$ dBHz and $T = 45$ dBHz).

$$w_1(x) = \begin{cases} 10^{\frac{x-T}{a}}\left(\left(A \times 10^{\frac{F-T}{a}} - 1\right)\frac{x-T}{F-T} + 1\right)^{-1}, & x < T \\ 1, & x \geq T \end{cases} \tag{30}$$

where

- x is the value of C/N_0 expressed in dBHz,
- T is a threshold after which the weight is set to 1 (indicating that the measurements are "good"),
- a allows the bending of the curve to be adjusted, as illustrated in Fig. 1,
- F defines the value of C/N_0 for which the function w_1 is forced to have the weight defined by parameter A
- A controls the value of the function w_1 for $x = F$ ($w_1(F) = 1/A$).

Fig. 1 displays typical evolutions of the weighting function w_1 for different values of a. As can be seen, this function equals 1 for the nominal value of C/N_0 ($\sim$ 45 dBHz) and is an increasing function of C/N_0 (mitigating the impact of the measurements associated with small values of C/N_0). Appropriate values of (T, a, F, A) in the weight function w_1 have to be determined. Multiple experiments allowed us to obtain $(T, a, F, A) = (45, 80, 20, 30)$ by cross-validation. Fig. 2 shows the variations of the estimated position RMSE as a function of one of these parameters (the other ones being fixed). As can be seen, the results are not very sensitive to the

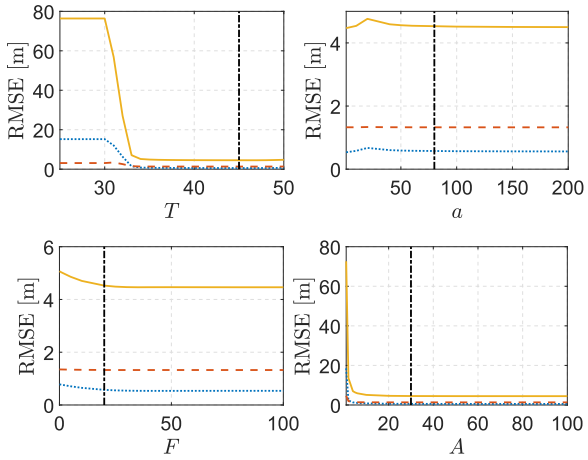

Fig. 2. Variations of the estimated RMSE versus (T, a, F, A): East (blue dotted), North (red dashed) and Up (yellow, continuous). Selected values are indicated by vertical black dot-dashed lines.

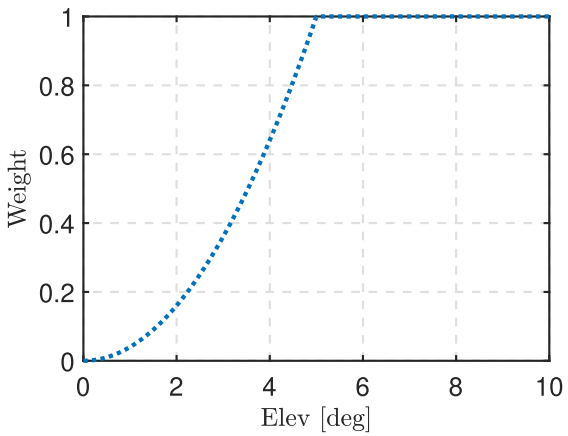

Fig. 3. Elevation weighting function w_2.

values of T, a, F and A providing these parameters are not too small.

A second important information that can be considered to mitigate the MP effects is related to the satellite elevations. It is very common [38] to define an elevation mask of 5 degrees, i.e., to exclude satellites with elevation lower than 5 degrees before computing the receiver position. However, in urban environment, it is important to preserve the largest number of satellite measurements. As a consequence, we propose to reduce the impact of satellites with low elevations without excluding them. There are many possibilities to define weighting functions satisfying this property. Following [54] and with the idea of penalizing satellites whose elevations are smaller than 5°, we consider the following weighting function

$$w_2(x) = \begin{cases} \dfrac{\sin^2(x)}{\sin^2(5°)} & x < 5° \\ 1 & x \geq 5° \end{cases} \tag{31}$$

which is displayed in Fig. 3.

The final weight introduced in the reweighted-ℓ_1 approach is defined as the product of the two previous functions for each satellite, i.e.,

$$w\left[(C/N_0)_i, e_i\right] = w_1\left[(C/N_0)_i\right] w_2(e_i) \tag{32}$$

where $(C/N_0)_i$ and e_i are the C/N_0 and elevation associated with the ith satellite. We also propose to assign the same weights for the ith pseudorange and ith pseudorange rate since these two measurements result from the same satellite, leading to $w_{N+i} = w_i$. Note that by construction the weights $w\left[(C/N_0)_i, e_i\right]$ belong to the interval $]0, 1]$. Finally, it is important to mention that the parameters C/N_0 and e are easily available at each receiver, since C/N_0 is directly estimated by the receiver and that the elevation can be computed using the actual and previous positions of each satellite (that are known thanks to the ephemeris contained in the navigation message).

V. Simulation Results

This section studies several experiments conducted with simulated and real data allowing the performance of the proposed algorithm to be appreciated.[2]

A. Synthetic Data

The synthetic data considered in this section have been generated using a reference position according to (10), and with noisy measurements resulting from (1) and (5). The sample size is $K = 500$ and 200 Monte Carlo runs have been considered for each scenario. In the first experiment, we have generated artificial additive biases, modelling multipath conditions, affecting pseudoranges and pseudorange rates between times instants $k = 50$ and $k = 150$ for satellite channels #1, #5 and #6. The bias amplitudes have been adjusted to 80, 60 and 40 meters for pseudoranges and to 5, 12 and 4 meters per seconds for pseudorange rates. Note that the satellite positions have been created from real ephemeris to work with realistic synthetic data. Additive noise was then generated (with $\sigma = 5$m for pseudoranges and $\sigma = 0.5\text{m.s}^{-1}$ for pseudoranges rate) in order to account for the receiver noise and the residual model errors (ionospheric, tropospheric, satellite clock, ephemeris and relativity). Finally, we generated C/N_0 uniformly between 45 dBHz and 48 dBHz in absence of MP, and between 30 dBHz and 33 dBHz in presence of MP (i.e., in channels #1, #5 and #6).

The proposed method was compared to the classical LASSO method, the reweighted-ℓ_1 algorithm [37] and our implementation of the coded filter [36]. The sparse method investigated in this work requires to tune the regularization parameter λ. Fig. 4 shows the RMSEs of the estimated position in the (East, North, Up) frame versus parameter λ. The value $\lambda = 1$ seems to provide to a good compromise between the RMSE value and the computation time for this example.

Figs. 5 and 6 show the estimated pseudorange and pseudorange rate biases for four representative channels. These figures show that the classical LASSO and reweighted ℓ_1 algorithms can potentially estimate biases in channels that are

[2]Matlab codes are available at http://perso.tesa.prd.fr/jlesouple/codes.html

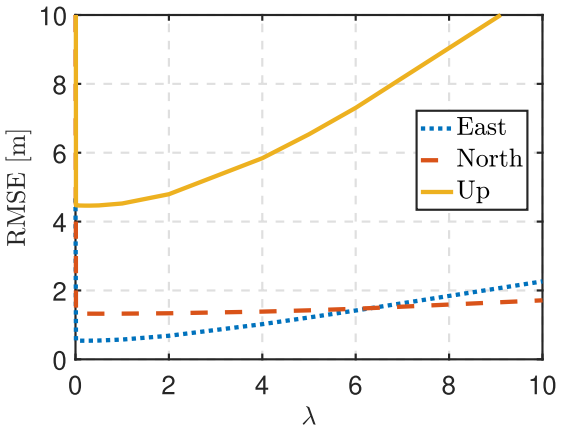

Fig. 4. RMSE of East North Up errors versus λ.

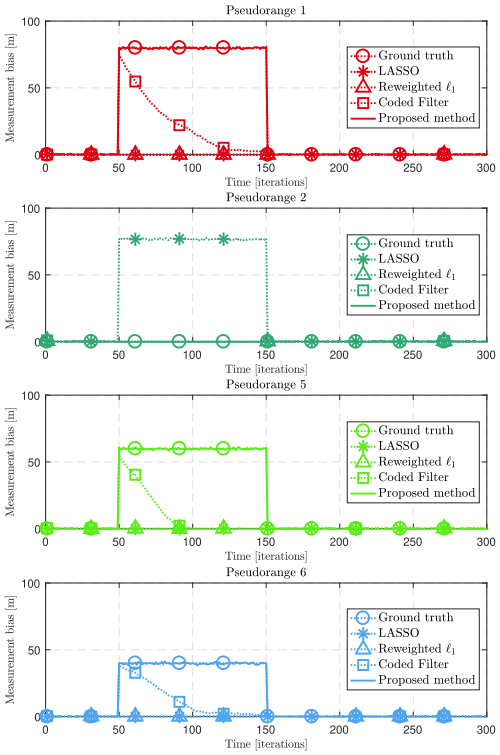

Fig. 5. Estimated bias and ground truth for representative pseudoranges.

not contaminated by MP, e.g., for the pseudorange of satellite #2, that they can also miss some channels affected by MP, as for the pseudorange of satellite #5, or can underestimate the bias value as for the pseudorange rate of satellite #5. This is no longer the case with the proposed reweighed ℓ_1 algorithm, which tends to estimate the biases more precisely. This conclusion is confirmed by the results of Fig. 7 showing the impact of proposed MP mitigation method on localization errors. Note that the robust Kalman filter described in [42] was also considered for this last comparison.

To summarize, the simulations conducted in the first part of this section show that the performance of the proposed algorithm are very satisfactory when the measurements and the state vector are in agreement with the measurement and state equations (10) and (12). The next sections consider experiments conducted with more realistic and real datasets.

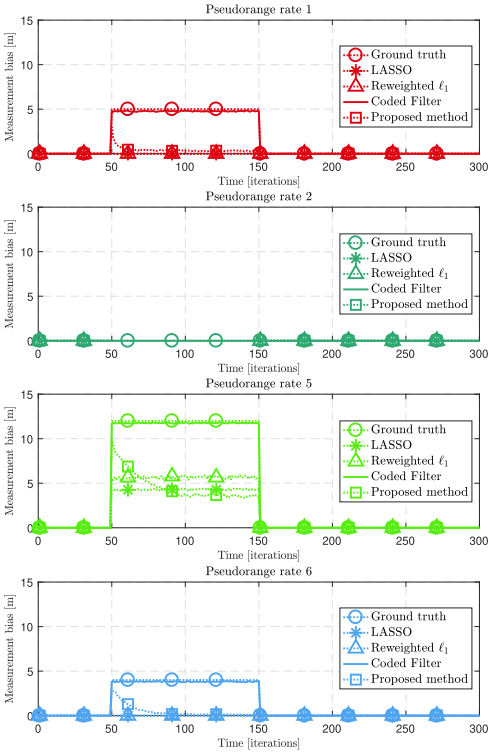

Fig. 6. Estimated bias and ground truth for representative pseudorange rates.

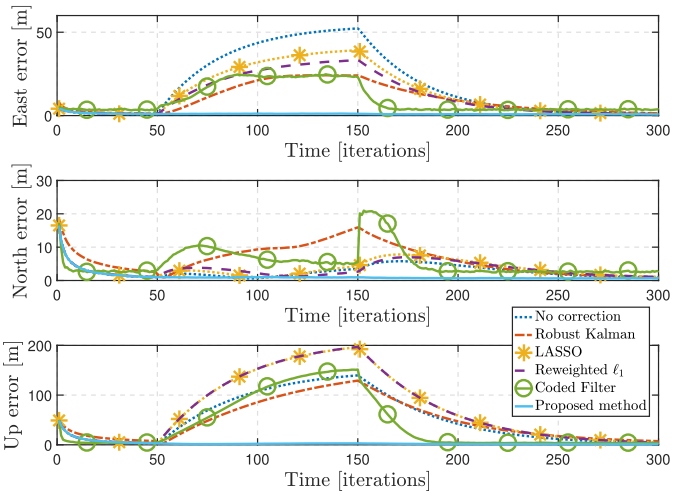

Fig. 7. Position root mean square errors (RMSEs) on each axis in the (East, Norh, Up) ENU frame without measurement corrections (dotted line), and with the proposed MP mitigation method (continuous line).

B. Realistic Data

This section studies a more realistic simulation scenario with a trajectory obtained from real data provided by a very accurate receiver (Novatel SPAN) (and no longer generated according to (10)) depicted in Fig. 8. The measurements associated with this trajectory have been generated using (12), and a bias has been added to the measurements of three satellites between the time instants $k = 200$ and 300 (with the same amplitudes as in the previous example). Fig. (9) displays the positioning errors obtained for this scenario. The performance of the proposed algorithm is similar to what was obtained using synthetic data, showing the algorithm

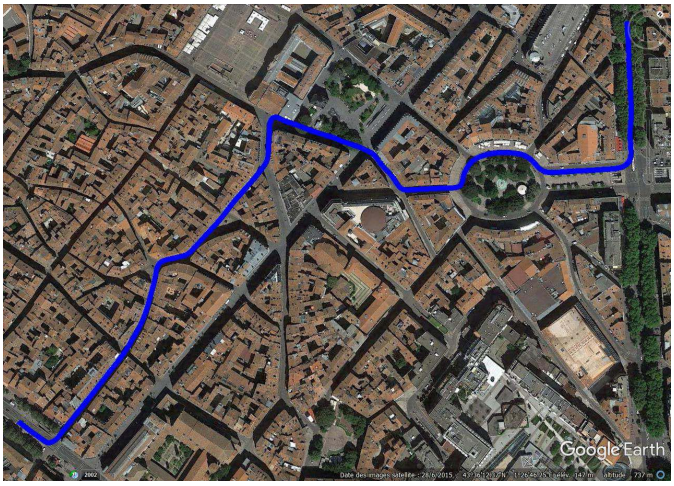

Fig. 8. Trajectory considered for the realistic dataset.

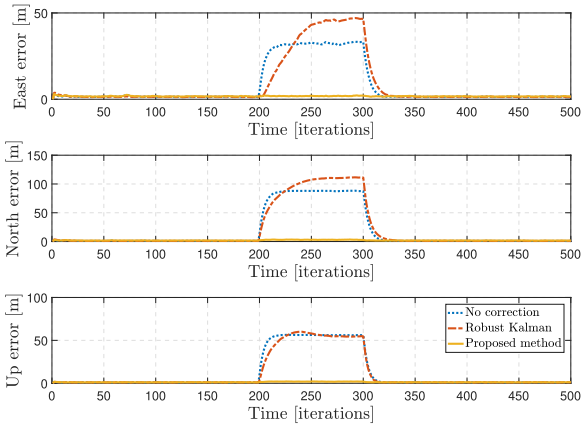

Fig. 9. Position RMSEs on each axis of the ENU frame without measurements corrections (dotted), for the REKF (dashed) and the proposed method (continuous).

robustness to a vehicle dynamics that does not exactly respect the state equation (10). The results illustrated in Fig. 10 allow us to appreciate the loss of performance obtained when the number of satellites affected by MP increases. The results obtained with the proposed sparse estimation method are satisfactory when there is less than 5 satellites out of 8 that are contaminated by MP. Conversely, the algorithm performance degrades significantly when the number of biased channels is larger than 6 out of 8, which defines the limit of the sparsity assumption for this simulation scenario, when too many satellites are affected by multipath.

C. Real Data

The proposed algorithm was finally evaluated on real measurements provided by a Ublox AEK-4T receiver, and compared with the robust EKF described in [42] and the Ublox solution. A reference solution was obtained during the measurement campaign using a very accurate (high-cost) receiver, i.e., a Novatel SPAN composed of a GPS receiver Propak-V3 and an inertial measurement unit (IMAR). The performance of the different algorithms is compared using

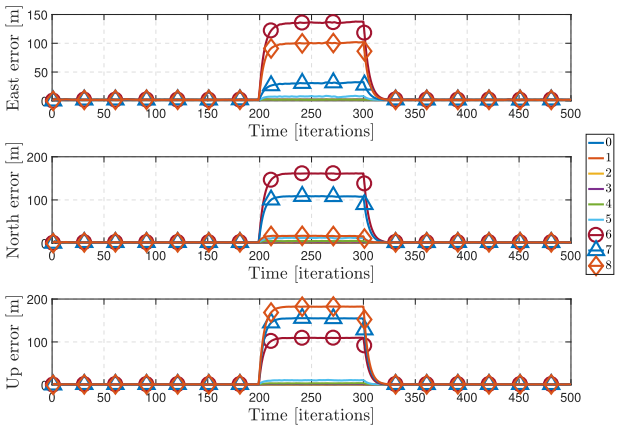

Fig. 10. Influence of the number of satellites affected by MP.

TABLE I

QUANTITATIVE RESULTS FOR THE HORIZONTAL AND VERTICAL ERRORS. (a) FULL CAMPAIGN, (b) OPEN SKY AND (c) URBAN ENVIRONMENT

	Horizontal Errors (m)			Vertical Errors (m)		
(a)	Min	Max	Med	Min	Max	Med
Ublox AEK 4-T	0.03	45.58	3.78	2.10^{-3}	22.73	10.05
REKF	0.03	64.67	4.92	0.03	106.10	6.03
Proposed method	0.03	47.22	3.43	6.10^{-4}	44.72	5.52
(b)	Min	Max	Med	Min	Max	Med
Ublox AEK 4-T	0.03	10.13	3.52	4.44	11.73	9.62
REKF	0.29	14.69	3.29	$7e^{-3}$	66.40	3.38
Proposed method	0.07	7.71	2.45	3.10^{-3}	6.95	3.46
(c)	Min	Max	Med	Min	Max	Med
Ublox AEK 4-T	0.59	24.96	4.73	0.01	22.73	10.25
REKF	0.24	32.22	11.65	0.01	53.80	12.59
Proposed method	0.04	31.69	6.90	9.10^{-4}	34.62	5.39

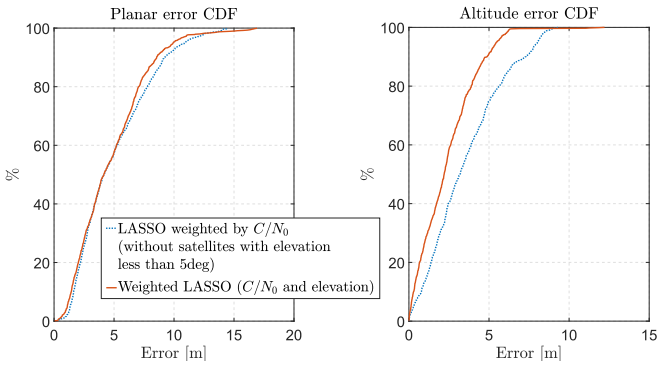

Fig. 11. Cumulative distribution functions of planar and altitude errors after weighting (continuous red) or discarding (blue dotted) low-elevation satellites.

data from the global campaign, but also using data resulting from specific portions of the trajectory corresponding to pretty clear sky and urban environment. Note that the Ublox receiver is a standalone receiver (it only uses its own GPS measurements to compute its position), and that its estimation algorithms used for positioning and computing the different measurements (correlators/discriminators) are not provided. The performance of the different methods is evaluated in terms of root mean square error (RMSE) for the different errors in the East, North and Up directions. The empirical cumulative distribution functions (cdfs) of these errors are

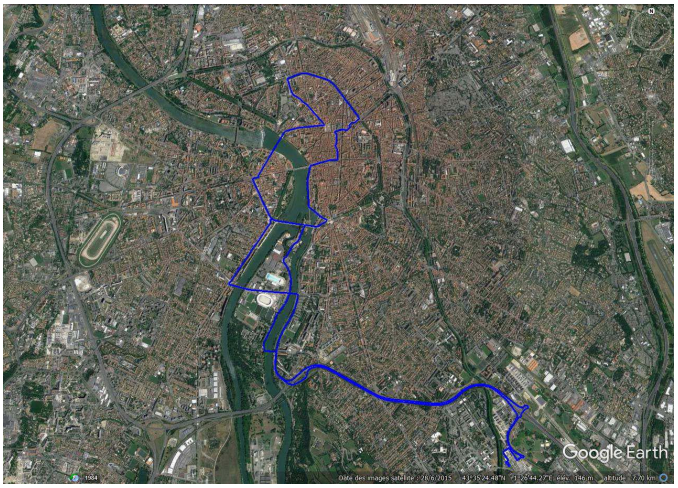

Fig. 12. Trajectory of the first real experiment plotted using Google Earth©.

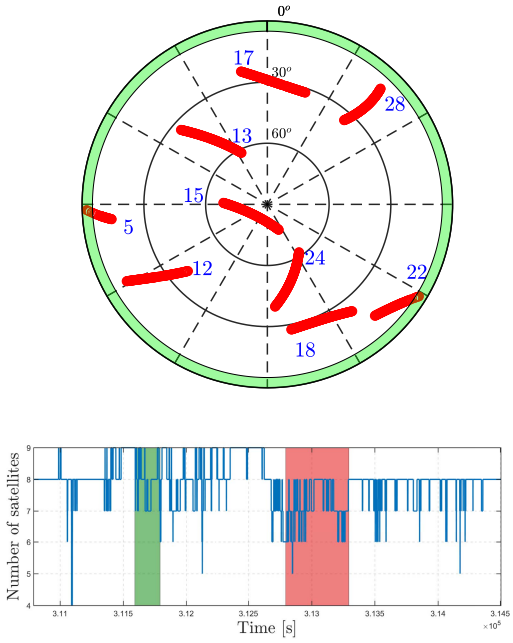

Fig. 13. Skyplot configuration (the green annulus represents elevations lower than 5°) and numbers of satellites all along the experiment. The green area corresponds to the "near open sky" scenario, and the red one is for the "urban" scenario.

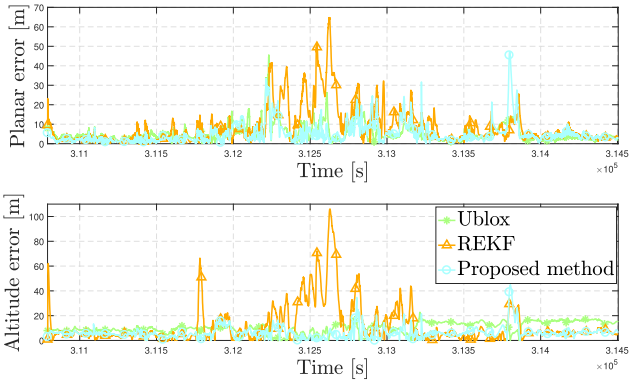

Fig. 14. Position error versus time for the Ublox solution, the REKF and the proposed method.

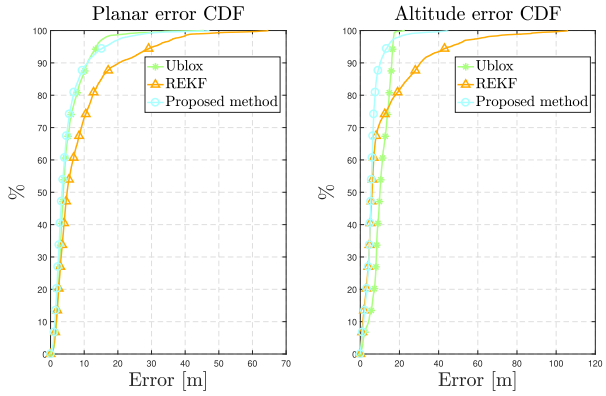

Fig. 15. Cumulative distribution functions of the position errors for the Ublox solution, the REKF and the proposed method.

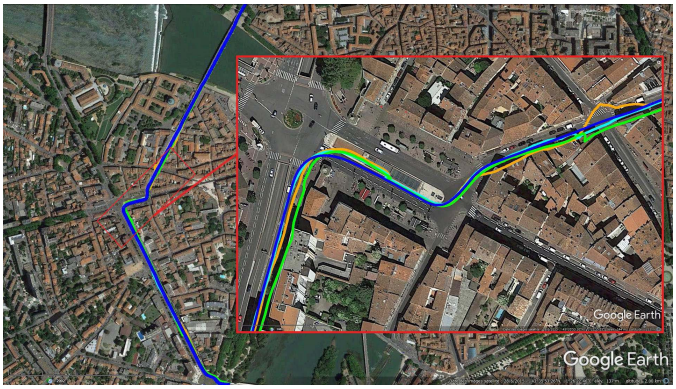

Fig. 16. Trajectory of the open sky scenario plotted using Google Earth©. The reference is in blue, the Ublox and REKF solutions are displayed in green and orange, whereas the proposed method is in cyan.

also shown for each method. We also decided to show the horizontal and altitude errors in the different figures. Finally, some quantitative results (minimum, maximum and median of horizontal and vertical errors) are summarized in Table I. These results confirm the good performance of the proposed sparse estimation algorithm.

1) Full Campaign: The trajectory considered during the full campaign is shown in Fig. 12 whereas the corresponding skyplot and numbers of satellites versus time are displayed in Fig. 13. Note that the trajectory contains some areas characterized by a quasi-constant number of satellites (equal to 8 or 9) and others where this number changes rapidly (between 5 and 8). Note also that only two satellites (#5 and #22) had sometimes an elevation lower than 5°, corresponding to the green annulus in Fig. 13. In order to appreciate the interest of the elevation constraint, we tested the performance of the proposed algorithm after discarding the satellites with elevation less than 5°(on a part of the whole trajectory). The corresponding cdfs are displayed in Fig. 11, showing that it is better to keep all the satellites including those with small elevation. Planar and altitude errors are shown in Fig. 14 whereas the corresponding cdfs can be observed in Fig. 15. The proposed method outperforms the REKF for both planar and altitude errors for this simulation scenario

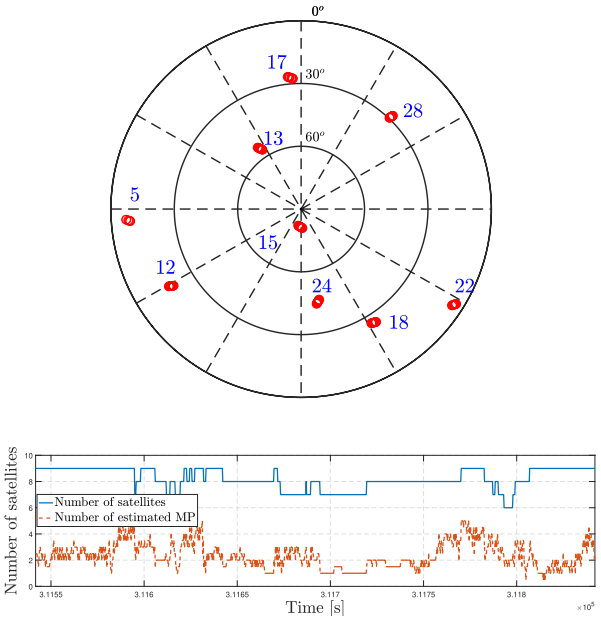

Fig. 17. Skyplot configuration and number of satellites for the open sky scenario.

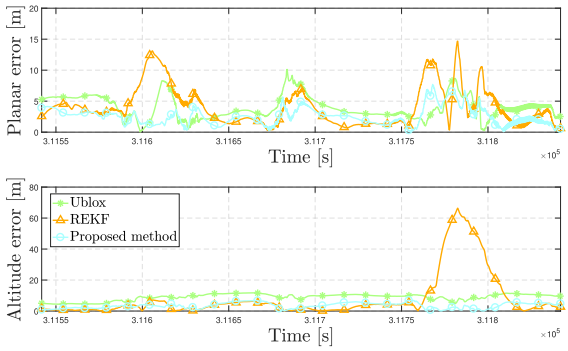

Fig. 18. Position errors versus time for the Ublox solution, the REKF and the proposed method for the open sky scenario.

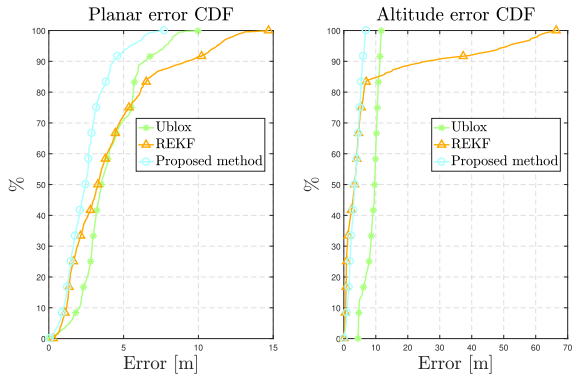

Fig. 19. Position error cumulative distribution functions for the Ublox solution, the REKF and the proposed method for the open sky scenario.

and seems to be competitive with respect to the Ublox built-in solution, at least for the full campaign. Table I confirms the good performance of the proposed sparse estimation method.

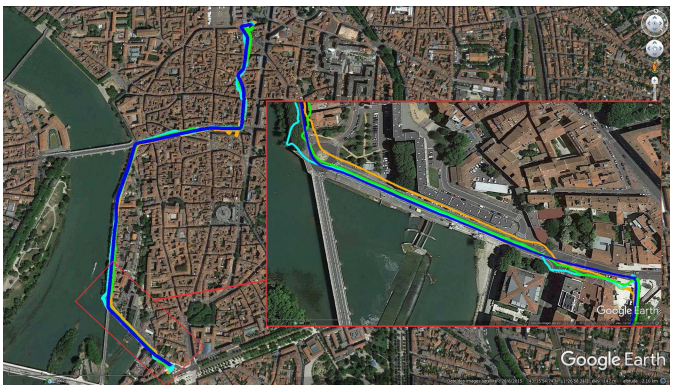

Fig. 20. Trajectory of the urban scenario plotted using Google Earth©. The reference is in blue, the Ublox and REKF solutions are in green and orange, whereas the proposed method is in cyan.

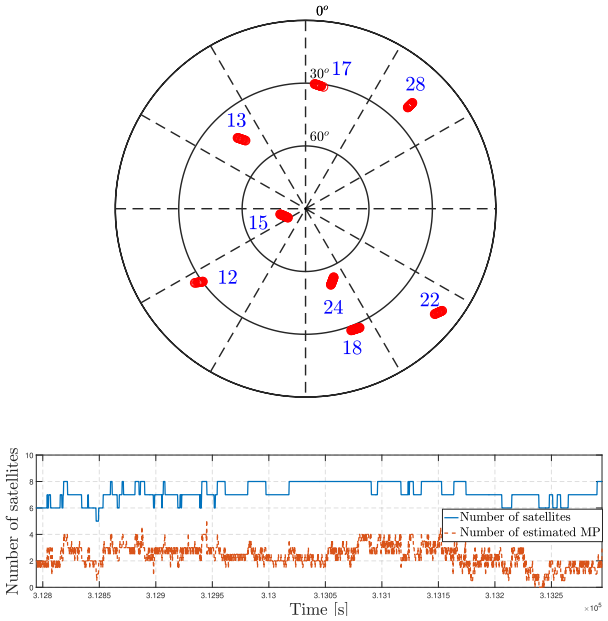

Fig. 21. Skyplot configuration and number of satellites for the urban scenario.

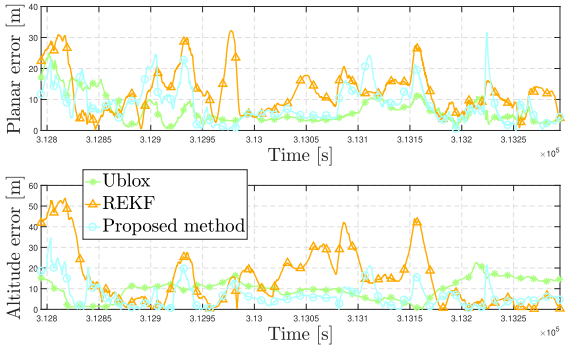

Fig. 22. Position errors versus time for the Ublox solution, the REKF and the proposed method for the urban scenario.

2) Light Urban: The trajectory corresponding to a "light urban" environment and the corresponding skyplot are depicted in Fig. 16 and Fig. 17. horizontal and altitude errors as well as the quantitative results of Table I show that the

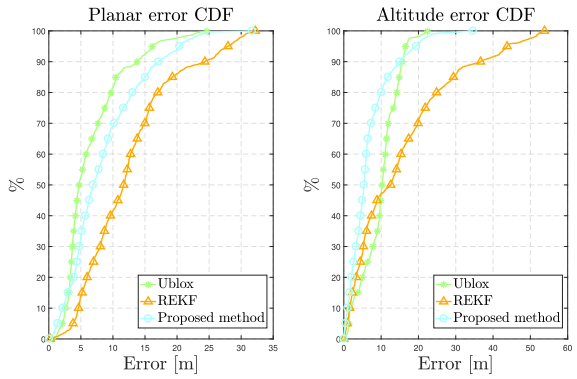

Fig. 23. Position error cumulative distribution functions for the Ublox solution, the REKF and the proposed method for the urban scenario.

proposed method outperforms both the Ublox and the REKF solutions for this clean environment.

3) Urban Canyon: The trajectory associated with the urban scenario and the corresponding sky plot are displayed in Figs. 20 and 21. The corresponding horizontal and altitude errors and their cdfs are displayed in Figs. 22 and 23, whereas some quantitative results are summarized in Table I. All these results show that the proposed method outperforms the REKF and performs similarly to the Ublox solution for this simulation scenario.

VI. Conclusions

This paper investigated a new GNSS estimation method exploiting the sparsity of channels affected by MP. We have shown via numerous experiments conducted on synthetic, realistic and real data that this method is very competitive with respect to more classical robust estimation strategies and to some extent to low-cost industrial solutions. The proposed method also showed some limits when the number of channels affected by multipath increased, i.e., when the sparsity assumption exploited by the proposed algorithm was no longer satisfied. Of course, the number of zero components of the MP vector is implicitly controlled by the value of the regularization parameter (since the value of this parameter allows the weights of the data fidelity and regularization terms to be balanced). However, investigating methods allowing this hyperparameter to be estimated directly from the data and from key parameters such as the average C/N_0 is clearly an important prospect. Methods based on the Stein risk [55] or on Markov chain Monte Carlo methods [56] would for instance deserve to be explored in the context of navigation using GNSS measurements. Another interesting future work concerns the automatic determination of the weight matrix used in the reweighted-ℓ_1 algorithm and the choice of the regularization enforcing sparsity of the MP components. Recent works conducted in [48] and [57] are clearly interesting to solve this issue. Finally another interesting point to investigate is the interest of the proposed method when coupled with other navigation algorithms, such as those adjusting the noise covariance matrix $\boldsymbol{R}_k$ adaptively [58] or using multiple models [59], or when the nature of the additive bias differs from multipaths.

Acknowledgments

The authors would like to thank M3Systems and the CNES for supporting this study and ISAE for providing the real data used in these experiments. They are also very grateful to Marcus Carlsson, Herwig Wendt and Thomas Oberlin for their fruitful discussions related to sparse estimation theory. This work is patented under [1].

References

[1] J. Lesouple, J.-Y. Tourneret, W. Vigneau, M. Sahmoudi, and F.-X. Marmet, "Traitement des Multitrajets GNSS par Méthode Parcimonieuse," French Patent FR1 753 907, May 3, 2017.

[2] O. Le Marchand, P. Bonnifait, J. Ibañez-Guzmán, D. Bétaille, and F. Peyret, "Characterization of GPS multipath for passenger vehicles across urban environments," *ATTI dell'Istituto Italiano di Navigazione*, no. 189, pp. 77–88, Jul. 2009.

[3] J. Marais, M. Berbineau, and M. Heddebaut, "Land mobile GNSS availability and multipath evaluation tool," *IEEE Trans. Veh. Technol.*, vol. 54, no. 5, pp. 1697–1704, Sep. 2005.

[4] B. W. Parkinson and J. J. Spilker, "Multipath effects," in *Global Positioning System: Theory and Applications* (Progress in Astronautics and Aeronautics), vol. 1, P. Zarchan, Ed. Washington, DC, USA: American Institute of Aeronautics & Astronautics, 1996, pp. 547–568, ch. 14.

[5] P. D. Groves, "Advanced Satellite Navigation," in *Principles of GNSS, Inertial, and Multisensor Integrated Navigation Systems*. Norwood, MA, USA: Artech House, 2008, pp. 279–302, ch. 8.

[6] M. T. Brenneman, Y. T. Morton, and Q. Zhou, "GPS multipath detection with ANOVA for adaptive arrays," *IEEE Trans. Aerosp. Electron. Syst.*, vol. 46, no. 3, pp. 1171–1184, Jul. 2010.

[7] S. Lee, E. S. Lohan, and S. Kim, "Array-based GNSS signal tracking with a reduced state signal model," *IEEE Trans. Aerosp. Electron. Syst.*, vol. 52, no. 3, pp. 1267–1283, Jun. 2016.

[8] S. Daneshmand, A. Broumandan, N. Sokhandan, and G. Lachapelle, "GNSS multipath mitigation with a moving antenna array," *IEEE Trans. Aerosp. Electron. Syst.*, vol. 49, no. 1, pp. 693–698, Jan. 2013.

[9] X. Chen, Y. Morton, and F. Dovis, "A computationally efficient iterative MLE for GPS AOA estimation," *IEEE Trans. Aerosp. Electron. Syst.*, vol. 49, no. 4, pp. 2707–2716, Oct. 2013.

[10] A. J. van Dierendonck, P. Fenton, and T. Ford, "Theory and performance of narrow correlator spacing in a GPS receiver," *Navigation*, vol. 39, no. 3, pp. 265–283, Sep. 1992.

[11] G. A. McGraw and M. S. Braash, "GNSS multipath mitigation using gated and high resolution correlator concepts," in *Proc. Nat. Tech. Meeting Inst. Navigat. (NTM)*, San Diego, CA, USA, Jan. 1999, pp. 333–342.

[12] B. R. Townsend and P. C. Fenton, "A practical approach to the reduction of pseudorange multipath errors in a LI GPS receiver," in *Proc. 7th Int. Tech. Meeting Satell. Division Inst. Navigat. (ION GPS)*, Salt Lake City, UT, USA, Sep. 1994, pp. 143–148.

[13] P. C. Fenton and J. Jones, "The theory and performance of NovAtel Inc.'s vision correlator," in *Proc. 19th Int. Tech. Meeting Satell. Division Inst. Navigat. (ION GNSS)*, Long Beach, CA, USA, Sep. 2005, pp. 2178–2186.

[14] R. D. J. van Nee, J. Siereveld, P. C. Fenton, and B. R. Townsend, "The multipath estimating delay lock loop: Approaching theoretical accuracy limits," in *Proc. IEEE Position Location Navigat. Symp.*, Apr. 1994, pp. 246–251.

[15] M. Sahmoudi and M. G. Amin, "Fast iterative maximum-likelihood algorithm (FIMLA) for multipath mitigation in next generation of GNSS receivers," in *Proc. 40th Asilomar Conf. Signals, Syst. Comput.*, Pacific Grove, CA, USA, Oct./Nov. 2006, pp. 579–584.

[16] N. Blanco-Delgado and F. D. Nunes, "Multipath estimation in multicorrelator GNSS receivers using the maximum likelihood principle," *IEEE Trans. Aerosp. Electron. Syst.*, vol. 48, no. 4, pp. 3222–3233, Oct. 2012.

[17] X. Chen, F. Dovis, S. Peng, and Y. Morton, "Comparative studies of GPS multipath mitigation methods performance," *IEEE Trans. Aerosp. Electron. Syst.*, vol. 49, no. 3, pp. 1555–1568, Jul. 2013.

[18] N. Jardak, A. Vervisch-Picois, and N. Samama, "Multipath insensitive delay lock loop in GNSS receivers," *IEEE Trans. Aerosp. Electron. Syst.*, vol. 47, no. 4, pp. 2590–2609, Oct. 2011.

[19] D. Bétaille, F. Peyret, M. Ortiz, S. Miquel, and L. Fontenay, "A new modeling based on urban trenches to improve GNSS positioning quality of service in cities," *IEEE Intell. Transp. Syst. Mag.*, vol. 5, no. 3, pp. 59–70, Jul. 2013.

[20] S. Peyraud *et al.*, "About non-line-of-sight satellite detection and exclusion in a 3D map-aided localization algorithm," *Sensors*, vol. 13, no. 1, pp. 829–847, 2013.

[21] A. Bourdeau, M. Sahmoudi, and J.-Y. Tourneret, "Constructive use of GNSS NLOS-multipath: Augmenting the navigation Kalman filter with a 3D model of the environment," in *Proc. 15th Int. Conf. Inf. Fusion (FUSION)*, Jul. 2012, pp. 2271–2276.

[22] S. Miura, L.-T. Hsu, F. Chen, and S. Kamijo, "GPS error correction with pseudorange evaluation using three-dimensional maps," *IEEE Trans. Intell. Transp. Syst.*, vol. 16, no. 6, pp. 3104–3115, Dec. 2015.

[23] Y. Gu, L.-T. Hsu, and S. Kamijo, "GNSS/onboard inertial sensor integration with the aid of 3-D building map for lane-level vehicle self-localization in urban canyon," *IEEE Trans. Veh. Technol.*, vol. 65, no. 6, pp. 4274–4287, Jun. 2016.

[24] P. Misra, B. P. Burke, and M. M. Pratt, "GPS performance in navigation," *Proc. IEEE*, vol. 87, no. 1, pp. 65–85, Jan. 1999.

[25] N. Alam and A. G. Dempster, "Cooperative positioning for vehicular networks: Facts and future," *IEEE Trans. Intell. Transp. Syst.*, vol. 14, no. 4, pp. 1708–1717, Dec. 2013.

[26] H. Ko, B. Kim, and S.-H. Kong, "GNSS multipath-resistant cooperative navigation in urban vehicular networks," *IEEE Trans. Veh. Technol.*, vol. 64, no. 12, pp. 5450–5463, Dec. 2015.

[27] P. D. Groves, "Fault detection and integrity monitoring," in *Principles of GNSS, Inertial, and Multisensor Integrated Navigation Systems*. Norwood, MA, USA: Artech House, 2008, pp. 451–470, ch. 15.

[28] S. Gleason and D. Gebre-Egziabher, "Indoor and weak signal navigation," in *GNSS Applications and Methods*. Norwood, MA, USA: Artech House, 2009, pp. 291–327, ch. 12.

[29] S. Zair, S. L. Hégarat-Mascle, and E. Seignez, "A-contrario modeling for robust localization using raw GNSS data," *IEEE Trans. Intell. Transp. Syst.*, vol. 17, no. 5, pp. 1354–1367, May 2016.

[30] N. Viandier, D. F. Nahimana, J. Marais, and E. Duflos, "GNSS performance enhancement in urban environment based on pseudo-range error model," in *Proc. IEEE/ION Position, Location Navigat. Symp.*, May 2008, pp. 377–382.

[31] F. Caron, M. Davy, A. Doucet, E. Duflos, and P. Vanheeghe, "Bayesian inference for linear dynamic models with Dirichlet process mixtures," *IEEE Trans. Signal Process.*, vol. 56, no. 1, pp. 71–84, Jan. 2008.

[32] A. Rabaoui, N. Viandier, E. Duflos, J. Marais, and P. Vanheeghe, "Dirichlet process mixtures for density estimation in dynamic nonlinear modeling: Application to GPS positioning in urban canyons," *IEEE Trans. Signal Process.*, vol. 60, no. 4, pp. 1638–1655, Apr. 2012.

[33] A. Giremus, J.-Y. Tourneret, and V. Calmettes, "A particle filtering approach for joint detection/estimation of multipath effects on GPS measurements," *IEEE Trans. Signal Process.*, vol. 55, no. 4, pp. 1275–1285, Apr. 2007.

[34] M. Leigsnering, F. Ahmad, M. G. Amin, and A. M. Zoubir, "Parametric dictionary learning for sparsity-based TWRI in multipath environments," *IEEE Trans. Aerosp. Electron. Syst.*, vol. 52, no. 2, pp. 532–547, Apr. 2016.

[35] M. Lasserre, S. Bidon, and F. Le Chevalier, "New sparse-promoting prior for the estimation of a radar scene with weak and strong targets," *IEEE Trans. Signal Process.*, vol. 64, no. 17, pp. 4634–4643, Sep. 2016.

[36] S. Mohiuddin, D. E. Gustafson, and Y. Rachlin, "Mitigating the effects of GNSS multipath with a coded filter," in *Proc. 24th Int. Tech. Meeting Satell. Division Inst. Navigat. (ION)*, Portland, OR, USA, Sep. 2011, pp. 2381–2394.

[37] E. J. Candès, M. B. Wakin, and S. P. Boyd, "Enhancing sparsity by reweighted ℓ_1 minimization," *J. Fourier Anal. Appl.*, vol. 14, nos. 5–6, pp. 877–905, 2008.

[38] P. D. Groves, "Satellite navigation systems," in *Principles of GNSS, Inertial, and Multisensor Integrated Navigation Systems*. Norwood, MA, USA: Artech House, 2008, pp. 161–194, ch. 6.

[39] P. D. Groves, "Satellite navigation processing, errors, and geometry," in *Principles of GNSS, Inertial, and Multisensor Integrated Navigation Systems*. Norwood, MA, USA: Artech House, 2008, pp. 195–278, ch. 7.

[40] B. Parkinson and J. Spilker, *Global Positioning System: Theory and Applications* (Progress in Astronautics and Aeronautics), vol. 163. Washington, DC, USA: AIAA, 1996.

[41] F. Gustafsson, *Statistical Sensor Fusion*. London, U.K.: Professional Publishing House, 2012.

[42] K. D. Rao, M. N. S. Swamy, and E. I. Plotkin, "GPS navigation with increased immunity to modeling errors," *IEEE Trans. Aerosp. Electron. Syst.*, vol. 40, no. 1, pp. 2–11, Jan. 2004.

[43] J. Lesouple, F. Barbiero, M. Sahmoudi, J.-Y. Tourneret, and W. Vigneau, "Multipath mitigation for GNSS positioning in urban environment using sparse estimation-supplementary materials," TéSA Lab., Toulouse, France, Tech. Rep., Jan. 2018. [Online]. Available: http://perso.tesa.prd.fr/jlesouple/documents/TRITS2018.pdf

[44] B. W. Remondi, "Computing satellite velocity using the broadcast ephemeris," *GPS Solutions*, vol. 8, no. 3, pp. 181–183, 2004.

[45] J. A. Klobuchar, "Ionospheric time-delay algorithm for single-frequency GPS users," *IEEE Trans. Aerosp. Electron. Syst.*, vol. AES-23, no. 3, pp. 325–331, May 1987.

[46] R. Leandro, M. C. Santos, and R. B. Langley, "UNB neutral atmosphere models: Development and performance," in *Proc. Inst. Navigat. Nat. Tech. Meeting (ION ITM)*, Jan. 2006, pp. 564–573.

[47] A. E. Niell, "Global mapping functions for the atmosphere delay at radio wavelengths," *J. Geophys. Res., Solid Earth*, vol. 101, no. B2, pp. 3227–3246, 1996.

[48] E. Soubies, L. Blanc-Féraud, and G. Aubert, "A continuous exact ℓ_0 penalty (CEL0) for least squares regularized problem," *SIAM J. Imag. Sci.*, vol. 8, no. 3, pp. 1607–1639, 2015.

[49] R. Tibshirani, "Regression shrinkage and selection via the lasso," *J. Roy. Statist. Soc. B, Methodol.*, vol. 58, no. 1, pp. 267–288, 1996.

[50] R. J. Tibshirani and J. Taylor, "The solution path of the generalized LASSO," *Ann. Statist.*, vol. 39, no. 3, pp. 1335–1371, Jun. 2011.

[51] S. Boyd, N. Parikh, E. Chu, B. Peleato, and J. Eckstein, "Distributed optimization and statistical learning via the alternating direction method of multipliers," *Found. Trends Mach. Learn.*, vol. 3, no. 1, pp. 1–122, Jan. 2011.

[52] T. Hastie, R. Tibshirani, and M. Wainwright, "The LASSO for Linear Models," in *Statistical Learning with Sparsity: The LASSO and Generalization* (C&H/CRC Monographs on Statistics & Applied Probability). Boca Raton, FL, USA: CRC Press, Apr. 2015, pp. 7–28, ch. 2.

[53] G. V. Pendse, "A tutorial on the LASSO and the 'shooting algorithm'," Harvard Med. School, Boston, MA, USA, Tech. Rep., Feb. 2011, vol. 13.

[54] E. Realini and M. Reguzzoni, "goGPS: Open source software for enhancing the accuracy of low-cost receivers by single-frequency relative kinematic positioning," *Meas. Sci. Technol.*, vol. 24, no. 11, p. 115010, 2013.

[55] S. Ramani, T. Blu, and M. Unser, "Monte-Carlo sure: A black-box optimization of regularization parameters for general denoising algorithms," *IEEE Trans. Image Process.*, vol. 17, no. 9, pp. 1540–1554, Sep. 2008.

[56] M. Pereyra *et al.*, "Tutorial on stochastic simulation and optimization methods in signal processing," *IEEE J. Sel. Topics Signal Process.*, vol. 10, no. 2, pp. 224–241, Mar. 2016.

[57] M. Carlsson. (Sep. 2016). "On convexification/optimization of functionals including an l2-misfit term." [Online]. Available: https://arxiv.org/abs/1609.09378

[58] P. D. Groves and Z. Jiang, "Height aiding, C/N_0 weighting and consistency checking for GNSS NLOS and multipath mitigation in urban areas," *J. Navigat.*, vol. 66, no. 5, pp. 653–669, 2013.

[59] R. Toledo-Moreo, M. A. Zamora-Izquierdo, B. Ubeda-Minarro, and A. F. Gomez-Skarmeta, "High-integrity IMM-EKF-based road vehicle navigation with low-cost GPS/SBAS/INS," *IEEE Trans. Intell. Transp. Syst.*, vol. 8, no. 3, pp. 491–511, Sep. 2007.

Julien Lesouple (S'17) was born in Arles, France. He received the degree in engineering from Ecole Nationale d'Ingénieurs de Constructions Aéronautiques, Toulouse, in 2014. He is currently pursuing the Ph.D. degree in signal processing with the TéSA Laboratory, National Polytechnic Institute of Toulouse, INP-ENSEEIHT, University of Toulouse. His Ph.D. study was supported by the CNES and M3 Systems. His research interests include GNSS, multipath mitigation, statistics, sparse representations, and Bayesian estimation.

Thierry Robert received the Ph.D. degree from National Polytechnic Institute of Toulouse in 1996. He is currently the Head of the Location/Navigation Signal and Time Frequency Department, Centre national d'études spatiales (CNES)—the French Space Agency. The department's activities cover signal design and processing, receivers and payloads involving location, and navigation systems including GNSS (Galileo and GNSS space receivers), search and rescue by satellite (Cospas-Sarsat and MEOSAR), and Argos. Other activities covered by the department is the time and frequency reference generation including the UTC (CNES) generation.

Mohamed Sahmoudi received the M.S. degree in statistics from Pierre-and-Marie-Curie University in 2000 and the Ph.D. degree in signal processing and communications from Paris-Sud University and Telecom Paris in 2004. While earning his Ph.D., he was an Assistant Lecturer with Ecole Polytechnique, then a Lecturer with Paris-Dauphine University. From 2005 to 2007, he was a Post-Doctoral Researcher on GPS signal processing with Villanova University, Radnor, PA, USA. In 2007, he joined the ETS School of Engineering, Montreal, Canada, to work on GNSS precise positioning. In 2009, he became an Associate Professor with the French Institute of Aeronautics and Space, Toulouse. His research interest includes weak multi-GNSS signals processing and multi-sensor fusion for navigation of cooperative and autonomous systems.

Jean-Yves Tourneret (SM'08) received the Ingénieur degree in electrical engineering from Ecole Nationale Supérieure d'Electronique, d'Electrotechnique, d'Informatique, d'Hydraulique et des Télécommunications (ENSEEIHT) de Toulouse in 1989 and the Ph.D. degree from National Polytechnic Institute, Toulouse, in 1992. He is currently a Professor with the ENSEEIHT, University of Toulouse, and also a Member of the IRIT laboratory (UMR 5505 of the CNRS). His research activities are centered around statistical signal and image processing with a particular interest to Bayesian and Markov chain Monte Carlo methods. He has been involved in the organization of several conferences including the European Conference on Signal Processing EUSIPCO'02 (program chair), the International Conference ICASSP'06 (plenaries), the Statistical Signal Processing Workshop SSP'12 (international liaisons), the International Workshop on Computational Advances in Multi-Sensor Adaptive Processing CAMSAP 2013 (local arrangements), the Statistical Signal Processing Workshop SSP'2014 (special sessions), and the Workshop on Machine Learning for Signal Processing MLSP'2014 (special sessions). He has been the General Chair of the CIMI workshop on optimization and statistics in image processing hold in Toulouse in 2013 (with F. Malgouyres and D. Kouam) and of the International Workshop on Computational Advances in Multi-Sensor Adaptive Processing CAMSAP 2015 (with P. Djuric). He has been a member of different technical committees including the Signal Processing Theory and Methods committee of the IEEE Signal Processing Society (2001-2007, 2010-2015). He has been serving as an Associate Editor for IEEE TRANSACTIONS ON SIGNAL PROCESSING (2008-2011, 2015-present) and has been an Associate Editor for *EURASIP Journal on Advances in Signal Processing* since 2013.

Willy Vigneau received the Engineering degree from Ecole Nationale Supérieure de l'Aéronautique et de l'Espace in 1999. He has been in charge of the Radionavigation Unit, M3 Systems, since 2002, and is especially managing project related to signal processing studies applied to GPS, EGNOS, and Galileo. He is currently the Technical Director of M3 Systems and is following M3 Systems' development on GPS, EGNOS, and Galileo algorithms and receivers. Recently, he has been particularly involved in several EGNOS and Galileo related projects as a Project Manager and as a Signal Processing Engineer.